Available online at www.sciencedirect.com

ScienceDirect

Journal of the European Ceramic Society 29 (2009) 1939–1945

www.elsevier.com/locate/jeurceramsoc

Slip casting of nanozirconia/MWCNT composites using a heterocoagulation process

Nere Garmendia[a], Isabel Santacruz[b,*], Rodrigo Moreno[b], Isabel Obieta[a]

[a] Unidad de Salud, INASMET-TECNALIA, 20009 San Sebastián, Spain
[b] Instituto de Cerámica y Vidrio, CSIC, 28049 Madrid, Spain

Received 28 August 2008; received in revised form 4 December 2008; accepted 12 December 2008

Abstract

The addition of carbon nanotubes (CNTs) is expected to increase the fracture toughness of ceramic matrix composites, but an uniform dispersion of the nanotubes in the matrix is essential. This is a complex issue in aqueous medium because of the nanotubes hydrophobicity. In this work, the stability and rheological behaviour of nanozirconia concentrated suspensions, from 20 to 33 vol% solids, with and without multiwall carbon nanotubes (MWCNTs) was optimised in order to obtain homogeneous green samples by slip casting. The manufacture of nanozirconia/MWCNTs composites was performed using a heterocoagulation process in which the CNTs were homogeneously coated by the ceramic particles through strong electrostatic attractive forces between the two phases and further consolidation by a slip casting route. After sintering, the effect of the MWCNT on the hardness and fracture toughness of the nanostructured zirconia samples was evaluated.

Keywords: Suspensions; Nanocomposites; Nanotubes; ZrO_2

1. Introduction

Many applications of ceramic matrix composites involve aggressive working environments or load solicitations so that mechanical properties such as fracture toughness or resistance to crack growth are of greatest importance. The incorporation of carbon nanotubes (CNTs) into a ceramic matrix is aimed to enhance the toughness of the material,[1] as in the case of fibre-reinforced ceramics. Since they were described by Iijima,[2] CNTs have become suitable reinforcing agents for many materials, including ceramics, due to their high aspect ratios and their unique mechanical properties. CNTs seem to be very attractive in the reinforcement of zirconia used for prostheses fabrication, improving the stiffness and avoiding the slow crack degradation and hence increasing the lifetime and reliability of the new material. Submicron-sized zirconia-based ceramics are widely used due to their excellent mechanical[3] or electrical properties[4] depending on the Y_2O_3 content. Partially stabilised zirconia has demonstrated to provide superior mechanical properties at room temperature. Such properties could be further enhanced by tailoring suitable nanostructures or by adding high efficiency reinforcing agents, such as the CNTs. However, both an uniform dispersion of the nanotubes and a homogeneous nanostructured matrix are essential. The great tendency to agglomeration of both the nanosized ceramic powders due to their high surface area, and the CNTs, on one hand, and the different aspect ratio between the nanotubes and the nanoparticles, on the other hand, strongly affect the preparation of a homogeneous mixture of the two phases within the nanocomposites. Nevertheless, the system YTZP/multiwall carbon nanotube (MWCNT) is receiving increased attention and several reports on this subject have been recently published.[5–8]

The colloidal processing approach allows to obtain well-dispersed CNTs-ceramic concentrated suspensions and the production of complex-shaped parts with a decreased number of flaws and smaller pores and higher reliability.[9] However, most wet forming routes, such as slip casting, in situ coagulation moulding, gel casting or tape casting, require stable slurries with high solids loading and low viscosity,[10–15] which are difficult to achieve with nanosized particles[16–18] and becomes more and more difficult as the shape factor increases, as in the case of CNTs.

---

* Corresponding author. Tel.: +34 91 735 58 40; fax: +34 91 735 58 43.
E-mail address: cruz@icv.csic.es (I. Santacruz).

0955-2219/$ – see front matter © 2009 Elsevier Ltd. All rights reserved.
doi:10.1016/j.jeurceramsoc.2008.12.014

Hence, the control of the interparticle forces and the modification of the particle surface are necessary to allow a good mixture of the two phases. This can be achieved by changing the surface charge, by coating the particles with an organic barrier layer or through the combination of the two, by means of polyelectrolytes.[19,20] The saturation adsorption and efficiency of polyelectrolytes strongly depend on their dissociation degree controlled by the pH.[21–23] It is known that changing the pH of stabilized concentrated suspensions from a pH regime with high surface potential towards the IEP through the addition of urea with catalyzers or lactones[11,24,25] produces the destabilization of the suspension; this procedure is the basis of the so-called Direct Coagulation Casting (DCC)[26–28] and is a method for the production of complex-shaped, high strength, high reliability ceramic components.

When two different species coexist in the suspension, each one showing a different isoelectric point, there is an intermediate pH zone where the two different species are oppositely charged. At this pH range, electrostatic attraction between them will occur thus leading to heterocoagulation.[29] This can lead to agglomeration when particles have similar size and shape. However, it has been demonstrated to be a suitable procedure to obtain core–shell structures and to coat bigger particles with smaller ones.[28,29] The coating of big non-spherical particles, such as the CNTs, in this way can be a valid option to maintain them stable and well-dispersed in a ceramic matrix.

The aim of this work was the manufacture of YTZP materials reinforced with a second phase of MWCNTs by a colloidal processing route based on the strong attractive interaction of the two phases by heterocoagulation.

2. Experimental procedure

As ceramic powder a commercial 3 mol% yttria tetragonal zirconia polycrystalline (YTZP) nanopowder from Inframat Advanced Materials (USA) was used. It has a primary particle size of 30–60 nm, and specific surface area of 41.7 m^2/g, as measured by one point nitrogen adsorption (Monosorb, Quantachrome, FL, USA).

MWCNTs supplied by Sunnano (China) were synthesized by Chemical Vapour Deposition (CVD) and had an average diameter between 10 and 30 nm, a length of 1–10 μm and a purity of over 80%, with a low metal content (0.85% Fe, 0.82% Ni and 1.07% Al). Atomic force microscopy (AFM) images of the powders were performed in a Digital Instruments Multimode AFM, Veeco, Santa Barbara, CA, with a Nanoscope III controller using tapping mode.

The zeta potentials of MWCNTs and YTZP were measured by laser Doppler velocimetry using a Zetasizer NanoZS (Malvern, UK) apparatus, although the authors know that this technique is not suitable for non-spherical particles. Measurements in this case were taken with cautions for comparison purposes. Suspensions were prepared to concentrations of 0.001 wt% using 10^{-2} M KCl solutions as electrolyte.

Concentrated ceramic suspensions were prepared according to the procedure reported elsewhere.[30] As deflocculant, aqueous solutions of an ammonium salt of polyacrylic acid-based polyelectrolyte (PAA, Duramax D3005, Rohm & Haas, USA) were prepared in deionised water to concentrations of 1.0–3.0 wt%. The amount of deflocculant added is expressed in terms of the active matter present in the dispersant with respect to suspension solids loading. Then, suspensions ranging from 60 wt% to 75 wt% (20–33 vol%) of nanosized YTZP were prepared. Tetramethylammonium hydroxide, TMAH (Aldrich-Chemie, Germany), supplied as a 25 wt% aqueous solution was added to the suspensions in order to obtain the desired value of pH (8.0 ± 0.1) although it also contributes to a better stabilisation of the suspensions.[26,30,31] The suspensions were homogenised using mechanical agitation with helices for 30 min and dispersed using a 400 W ultrasound probe (UP400S, Hielscher Ultrasonics GmbH, Stuttgart, Germany). Suspensions were cooled in an ice-water bath during ultrasonication (US) in order to avoid excessive heating. Ultrasonication was applied on small amounts of suspensions each time, 20 mL, for total times of 2–8 min using 2 min steps separated by 15 min mechanical stirring. The rheological behaviour of the suspensions with different solid loadings and different ultrasonication times was studied in order to optimize the solids loading and to reach increased green densities. The measurements were performed using a rheometer (Model RS50, Thermo Haake, Karlsruhe, Germany) with a double-cone and plate system (60 mm in diameter, 2° cone angle) provided with a solvent trap to reduce evaporation. A three-stage measuring program with a linear increase in the shear rate from 0 to 1000 s^{-1} in 300 s, a plateau at 1000 s^{-1} for 120 s, and a further decrease to zero shear rate in 300 s was used. The maximum packing fraction of the nanosized YTZP was predicted using the Krieger–Dougherty model.

To obtain the composites, nanosized YTZP suspensions were prepared to 65 wt% solids adding 0.3 wt% of MWCNTs with regard to the YTZP mass, that is a volume fraction of 0.24 (1.0 vol% of MWCNTs).

The dispersion state of the MWCNTs was improved by the adsorption of a cationic dispersant, namely poly(ethylenimine) (PEI), which provides a positive charge to the MWCNTs at the working pH (8.0 ± 0.1). The suspensions were prepared by adding 20 wt% PEI (Aldrich Chemical Company, USA) to deionised water prior to the addition of the MWCNTs and sonication for 2 min. Then, the desired amount of polyelectrolyte and the YTZP powders were added and the new suspension was ultrasonicated for further 8 min.

The rheological behaviour of the YTZP/MWCNTs suspension was studied in the same way as the YTZP suspensions. Slip-cast samples of YTZP with and without MWCNTs with 9 mm in diameter and 10 mm in thickness were obtained and were left to dry for 24 h at room conditions.

The green densities of the cast bodies were measured by the Archimedes' method in mercury. Theoretical densities of 6.10 and 6.06 $g\,cm^{-3}$ were considered for the YTZP and the YTZP/MWCNTs, respectively. Green fracture surfaces were observed by field emission gun scanning electron microscopy, FEG-SEM (LEO 1530VP, LEO Elektronenmikroskopie GmbH, Oberkochen, Germany). Dynamic sintering tests were performed on the YTZP and YTZP/MWCNTs samples in Argon up to 1500 °C with a heating rate of 5 °C/min using a differential dilatometer (Setaram, Setsys TMA-18, Caluire, France). The specimens were sintered at 1350 °C/1 h. The final densities were measured using the Archimedes' method in water. The fracture surfaces were observed by SEM (JEOL JSM-5910-LV, Tokyo, Japan) and the grain size was measured on SEM pictures.

The hardness and the fracture toughness of the samples were measured using the Vickers indentation method. The indentation tests were performed with a load of 5 kg, according to the UNE-EN ISO 6507-1:2006 standard. The fracture threshold (K_{I0}) was calculated by measuring the crack length some days after the indentation, once the crack had reached the Griffith equilibrium, as it is a more "intrinsic" value of the material. For ceramic joint prostheses, this threshold determines a safety range of use: the higher the threshold, the higher the reliability and consequently the lifetime.[32] It was determined according to the Lawn's expression[33]:

$$K_{I0} = \chi \; P c_0^{-3/2} \tag{1}$$

$$\chi = C \left(\frac{E}{H}\right)^{1/2} \tag{2}$$

where P is the applied force (N), c_0 is the crack length (m). χ is a constraint factor defined by Anstis et al.,[34] where C is a geometric constant that takes the value of 0.016, H is the Vickers hardness (GPa) and E is the Young's modulus (GPa). As a basic approach, the Young's modulus was assumed to be $E = 220$ GPa for all the samples, irrespective of their composition. Although indentation toughness method is controversial, especially in CNT composites,[35–37] it is still a very common method used for zirconia ceramics and zirconia composites.[5,7,8,32]

3. Results and discussion

Fig. 1 shows AFM micrographs of the starting nanosized YTZP powders and MWCNTs. The YTZP seems to be free of agglomerates. The nanotubes show an average width of nanometers and a typical length shorter than 1 μm.

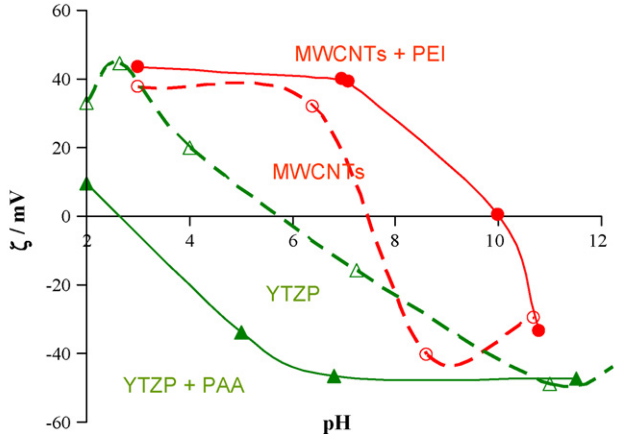

Fig. 2. Comparison of the zeta potential as a function of pH for YTZP, MWCNTs, YTZP with 2% wt PAA and MWCNTs with 20 wt% PEI.

Fig. 2 shows the evolution of the zeta potential with pH for YTZP and MWCNTs with and without their corresponding deflocculants (PAA and PEI for the ceramic particles and the nanotubes, respectively). From that figure, it can be seen that when no surfactant or polyelectrolyte are used, there is a narrow range of pH (from 6 to less than 8) where heterocoagulation can occur, making difficult the controlled adsorption of the nanoparticles on the nanotubes. When using dispersant with different surface charge, it is possible to increase the range of heterocoagulation to near 7 units of pH, viz. from pH 3 to pH 10, thus allowing a simple control of the heterocoagulation process.

The zeta potential values of diluted YTZP suspensions with 1.0, 2.0 and 3.0 wt% polyelectrolyte were −37 ± 6, −37 ± 9, and −35 ± 12, respectively. A concentration of 2.0 wt% deflocculant was selected to prepare the concentrated suspensions, in order to assure complete coverage. YTZP suspensions were prepared in concentrations ranging from 60 to 75 wt% (20–33 vol%). The influence of the addition of TMAH was first studied on 60 wt% suspensions. Fig. 3(a) shows the flow curves of the suspensions at that solids loading with and without

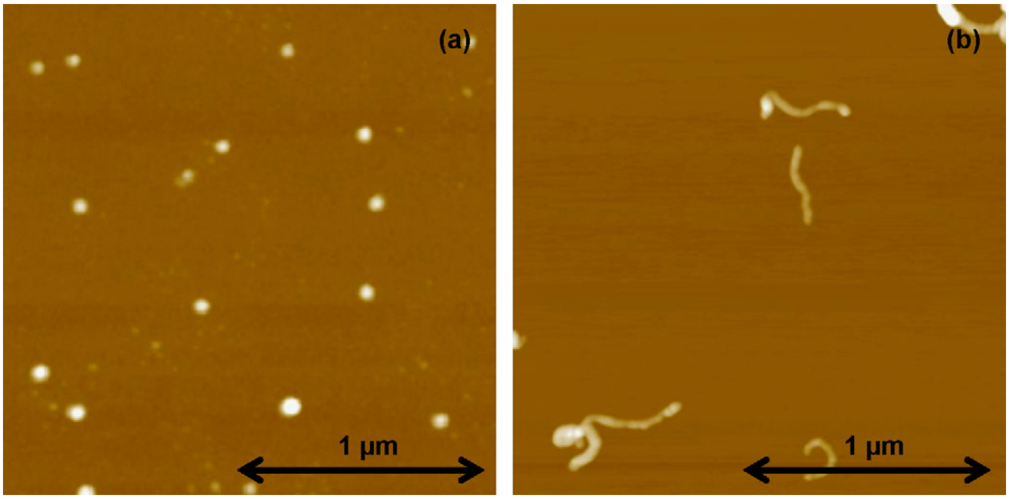

Fig. 1. AFM images of the of the YTZP (a) and the MWCNTs (b).

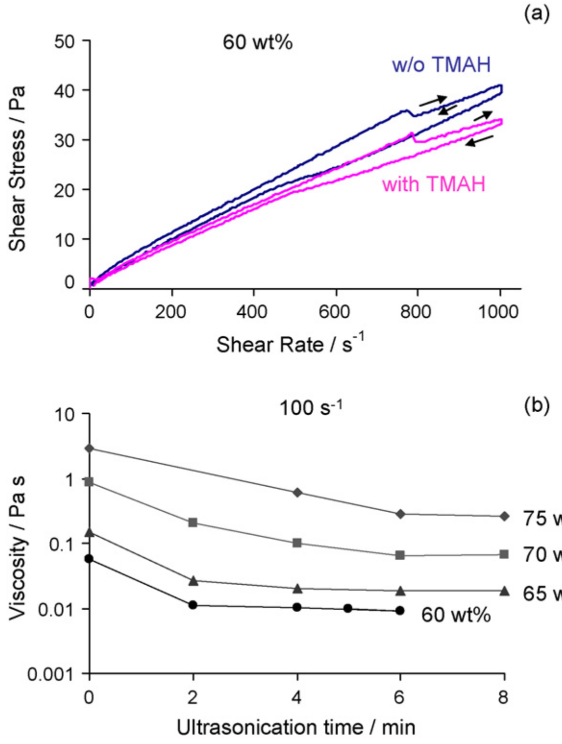

Fig. 3. Flow curves of 60 wt% suspensions with 2 wt% PAA with and without TMAH with no ultrasonication (a), and evolution of the viscosity with ultrasonication time for the concentrated YTZP suspensions (60–75 wt%) with 2 wt% PAA and TMAH. Shear rate: 100 s^{-1} (b).

TMAH prepared with PAA and without ultrasound treatment. Both suspensions were thixotropic although the viscosity of the former decreased due to the better stabilization.[30,31,38–40] For this reason, TMAH was added in the preparation of the nanozirconia suspensions. The suspensions with PAA and TMAH were homogenized by using an ultrasound probe for a few minutes. The evolution of the viscosity of the 60, 65, 70 and 75 wt% suspensions with different US times was studied by taking the viscosity value of each suspension at 100 s^{-1} from the up-curves. This evolution is shown in Fig. 3(b), where the viscosity of the suspensions after ultrasonication decreased due to the stabilization achieved when the agglomerates break down, even after only 2 min US. The optimum viscosity and thixotropy were reached for ultrasonication times of 6–8 min. The deflocculant content of the concentrated suspensions (75 wt%, 33 vol%) was later increased up to 2.7 wt%, but the viscosity of this suspension was very high, even after 8 min ultrasonication, so that 2 wt% PAA was maintained as the most effective concentration of polyelectrolyte even for the concentrated YTZP suspensions.

The variation of the relative viscosity as a function of the volume fraction of solids and the time of ultrasonication mixing was studied. The experimental data were fitted to the cross model that provides the high shear limiting viscosity (η_∞). The evolution of viscosity with volume fraction of solids was then fitted to the Krieger–Dougherty equation, to predict the maximum packing fraction (ϕ_m),[41] as it is shown in Fig. 4 for different US mixing times. As expected, from 0 to 6 min, the higher the ultrasonication time the higher the value of ϕ_m. Without ultrasound treatment, ϕ_m was 0.34, but ultrasonication times of up to 6 min resulted in $\phi_m = 0.4$.

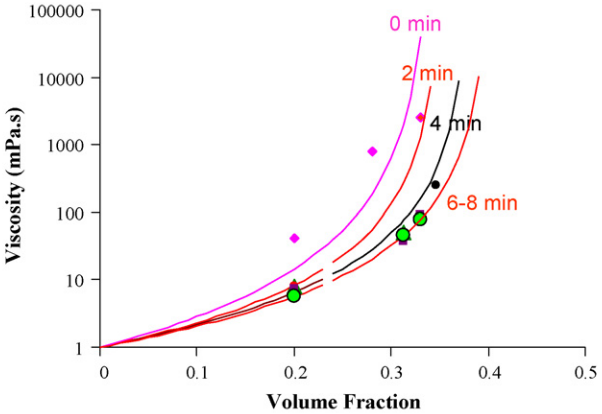

Fig. 4. Limit viscosity (η_∞) as a function of the volume fraction and the ultrasonication time.

Once the dispersion of the YTZP was optimised, the MWCNTs were added to the suspensions. It can be expected that after the addition of the nanotubes to the suspensions the maximum packing fraction would be reduced, due to the dimensions/shape of the MWCNTs. Fig. 5 shows the flow curves of the 65 wt% YTZP suspension (with 2 wt% PAA and 6 min ultrasound) with and without MWCNTs. The addition of the nanotubes has a strong effect on the viscosity and a broad hysteresis cycle appears. The density values of the corresponding green samples are shown in Table 1.

FEG-SEM fracture surfaces of the green YTZP and YTZP/MWCNTs samples are shown in Fig. 6. From these micrographs it can be seen that homogeneous green bodies were obtained in both cases. For the YTZP/MWCNTs green samples, the carbon nanotubes are homogeneously distributed and no bundles or agglomerates are observed.

In order to select the sintering cycle, dilatometric tests were performed for both samples, Fig. 7. The micrographs of the sintered samples are shown in Fig. 8, where the YTZP sample (Fig. 8a) shows larger grain size than the YTZP/MWCNTs sample (Fig. 8b). This is believed to be a consequence of the incomplete densification of samples containing nanotubes, in

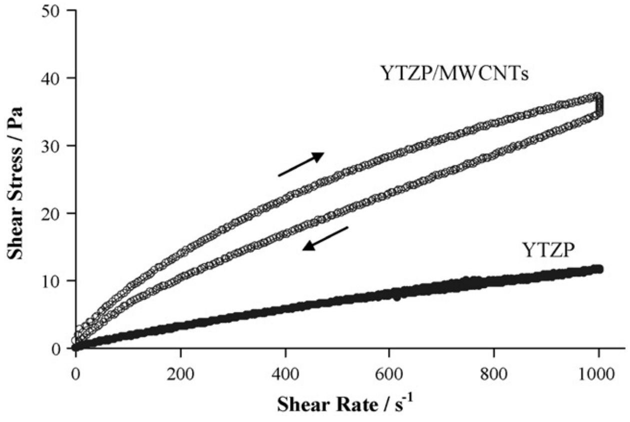

Fig. 5. Flow curves of 65 wt% YTZP suspensions with 2 wt% PAA and 65 wt% YTZP/MWCNTs.

Table 1
Physical and mechanical properties of the YTZP and YTZP/MWCNTs samples.

	Density		Grain size/nm			Vickers hardness/ GPa ±0.1	Fracture threshold (K_{I0})/ MPa m$^{1/2}$ ±0.1
	Green ± 0.2	Sintered ± 0.1	Min.	Max.	Average		
YTZP	2.8 g cm^{-3} (45.9%TD)	5.9 g cm^{-3} (96.7%TD)	180	770	435	12.5	3.8
YTZP/MWCNTs	2.6 g cm^{-3} (42.9%TD)	5.8 g cm^{-3} (95.7%TD)	100	370	220	11.0	4.0

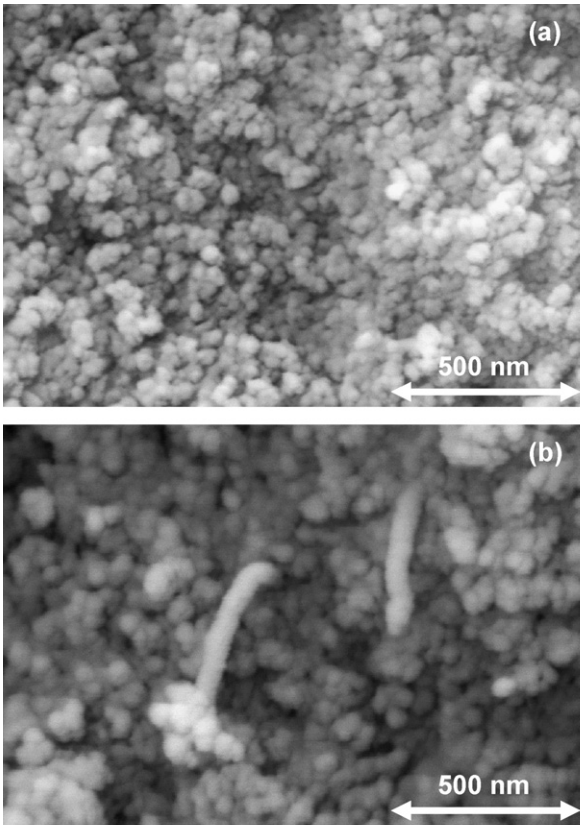

Fig. 6. Green nanostructure of slip cast nanosuspensions: (a) YTZP and (b) YTZP/MWCNTs.

agreement with the dilatometry (Fig. 7), which shows that the maximum shrinkage is smaller for the composite. In Table 1 the final densities and the grain sizes of the sintered samples are presented. The obtained density is larger for the YTZP, nearly 97% TD, while that of YTZP/MWCNTs is nearly 96% TD. The values of the Vickers hardness and fracture toughness are also presented in Table 1. With the addition of the nanotubes, a decrease of the hardness of 12.5% is produced, which is explained by the lower density of the nanocomposite and the addition of a softer phase to the system. On the other hand, it is observed that a small amount of carbon nanotubes (1 vol%) leads to an increase of the fracture toughness of 6.4%. Although this is not a great enhancement it opens the path for a new kind of nanocomposites with better fracture toughness. Anyhow, it will be necessary to obtain final YTZP/MWCNTs composites with a density above 97% if we want to use them for load bearing applications that require good mechanical properties. In previous works[42] we have described the procedure to obtain nanozirconia partially coated MWCNTs, where the formation of Zr–C compounds is reported. These coated MWCNTs offer a better wettability in the zirconia matrix and ensure a good load transfer among the zirconia matrix and the nanotubes due to the interfacial bonding. Furthermore, as they are coated, they will not behave as a source of defects in the matrix and good final densities are expected. This issue will be studied in future work.

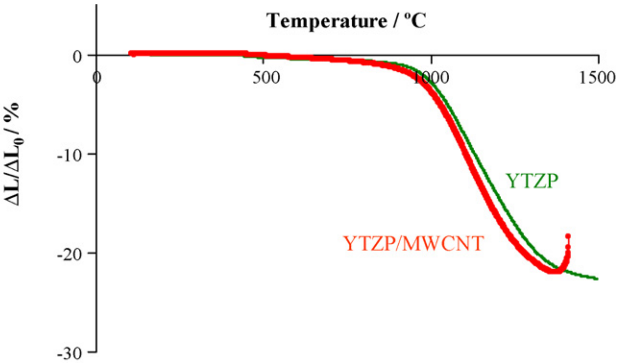

Fig. 7. Dilatometries of YTZP and YTZP/MWCNTs.

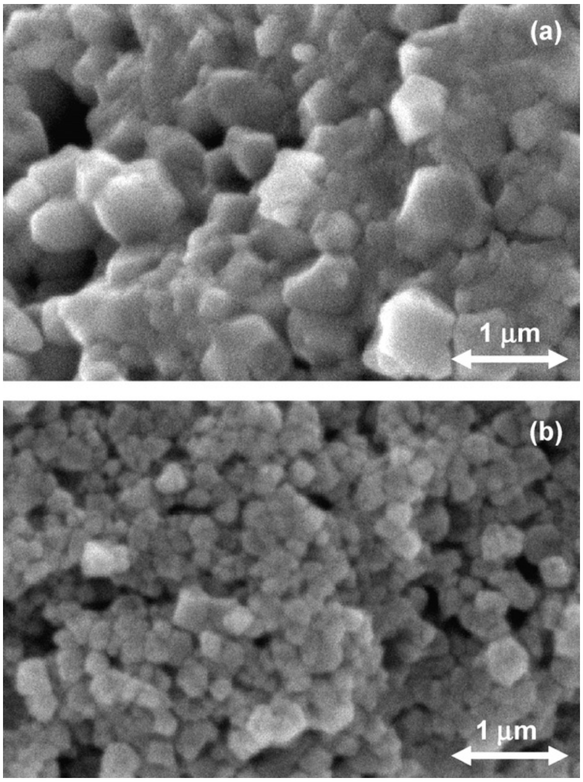

Fig. 8. Sintered nanostructure of slip cast nanosuspensions: (a) YTZP and (b) YTZP/MWCNTs.

4. Conclusions

YTZP and YTZP/MWCNTs aqueous nanosuspensions with up to 33 vol% solids loading have been prepared by ultrasonication and the addition of different deflocculants. The selected deflocculants were successfully adsorbed onto the particles and nanotubes, and hence, the heterocoagulation process seems to help in obtaining green samples. The maximum volume fraction increases with increasing ultrasonication time under the range of study. The presence of MWCNTs in the ceramic nanosuspensions affects homogenisation since both viscosity and hysteresis cycle increases; hence it is necessary to reduce the solids loading of the suspension. The addition of carbon nanotubes affects also the total densification of the samples, because they act as a source of defects in the matrix, and a decrease of the hardness occurs. Since the fracture toughness slightly increases, it suggests that carbon nanotubes could be strengthening agents for zirconia-based materials. To preserve the hardness of the ceramic matrix and increase the toughness it will be necessary to ensure a good load transfer among the zirconia matrix and the nanotubes. This goal may be achieved by using nanozirconia partially coated carbon nanotubes that offer an interfacial bonding between the zirconia and the MWCNTs. This subject will be studied in future work.

Acknowledgements

The authors thank the Basque Government (PI-2004-2, BF105.R2.555 and Etortek: Nanomaterials) for its financial support. This work has been partially supported by the Spanish Ministry of Science and Innovation through projects MAT2006-13480 and MAT2006-01038. Dr. I. Santacruz thanks ESF and CSIC for the concession of a postdoctoral contract I3P-PC2005L.

References

1. Curtin, W. A. and Sheldon, B. W., CNT-reinforced ceramics and metals. *Mater. Today*, 2004, **7**, 44–49.
2. Iijima, S., Helical microtubules of graphitic carbon. *Nature*, 1991, **354**, 56–58.
3. Kondoh, J., Shiota, H., Kawachi, K. and Nakatani, T., Yttria concentration dependence of tensile strength in yttria-stabilized zirconia. *J. Alloys Compd.*, 2004, **365**, 253–258.
4. Kosacki, I., Suzuki, T., Petrovsky, V. and Anderson, H. U., Electrical conductivity of nanocrystalline ceria and zirconia thin films. *Solid State Ionics*, 2000, **136–137**, 1225–1233.
5. Sun, J., Gao, L., Iwasa, M., Nakayama, T. and Niihara, K., Failure investigation of carbon nanotube/3Y-TZP nanocomposites. *Ceram. Int.*, 2005, **31**, 1131–1134.
6. Ukai, T., Sekino, T., Hirvonen, A., Tanaka, N., Kusunose, T., Nakayama, T. and Niihara, K., Preparation and electrical properties of carbon nanotubes dispersed zirconia nanocomposites. *Key Eng. Mater.*, 2006, **317–318**, 661–664.
7. Duszová, A., Dusza, J., Tomásek, K., Morgiel, J., Blugan, G. S. and Kübler, J., Zirconia/carbon nanofiber composite. *Scripta Mater.*, 2008, **58**, 520–523.
8. Duszová, A., Dusza, J., Tomásek, K., Blugan, G. S. and Kübler, J., Microstructure and properties of carbon nanotube/zirconia composite. *J. Eur. Ceram. Soc.*, 2008, **28**, 1023–1027.
9. Lange, F., Powder processing science and technology for increased reliability. *J. Am. Ceram. Soc.*, 1989, **72**, 3–15.
10. Wang, L. A. and Aldinger, F., Near net shape forming of advanced ceramics. *Adv. Eng. Mater.*, 2000, **3**, 110–113.
11. Binner, J. G. P., Santacruz, I. and Mc. Dermott, A. M., Rheological characterization of electrosterically dispersed alumina suspensions during in-situ coagulation. *J. Am. Ceram. Soc.*, 2006, **89**, 863–868.
12. Sigmund, W. M., Bell, N. S. and Bergström, L., Novel powder-processing methods for advanced ceramics. *J. Am. Ceram. Soc.*, 2000, **83**, 1557–1574.
13. Santacruz, I., Nieto, M. I. and Moreno, R., Alumina bodies with near-to-theoretical density by aqueous gelcasting using concentrated agarose solutions. *Ceram. Int.*, 2005, **31**, 439–445.
14. Lewis, J. A., Colloidal processing of ceramics. *J. Am. Ceram. Soc.*, 2000, **83**, 2341–2359.
15. Moreno, R., The role of slip additives in tape-casting technology: part I—solvents and dispersants. *Am. Ceram. Soc. Bull.*, 1992, **71**, 1521–1530.
16. Shan, H. B. and Zhang, Z. T., Slip casting of nanometre-sized tetragonal zirconia powder. *Br. Ceram. Trans.*, 1996, **95**, 35–38.
17. Meier, L. P., Urech, L. and Gauckler, L. J., Tape casting of nanocrystalline ceria gadolinia powder. *J. Eur. Ceram. Soc.*, 2004, **24**, 3753–3758.
18. Boschini, F., Guillaume, B., Rulmont, A., Cloots, R. and Moreno, R., Slip casting of barium zirconate aqueous concentrated suspensions. *J. Eur. Ceram. Soc.*, 2006, **26**, 1591–1598.
19. Cesarano III, J. and Aksay, I. A., Stability of aqueous α-Al_2O_3 suspensions with poly(methacrylic acid) polyelectrolyte. *J. Am. Ceram. Soc.*, 1988, **71**, 250–255.
20. Cesarano III, J. and Aksay, I. A., Processing of highly concentrated aqueous α-alumina suspensions stabilized with polyelectrolytes. *J. Am. Ceram. Soc.*, 1988, **71**, 1062–1067.
21. Guo, L. C., Zhang, Y., Uchida, N. and Uematsu, K., Adsorption effects on the rheological properties of aqueous alumina suspensions with polyelectrolyte. *J. Am. Ceram. Soc.*, 1998, **81**, 549–556.
22. Davies, J. and Binner, J. G. P., The role of ammonium polyacrylate in dispersing concentrated alumina suspensions. *J. Eur. Ceram. Soc.*, 2000, **20**, 1539–1553.
23. Sun, J., Gao, L. and Guo, J., Influence of the initial pH on the adsorption behaviour of dispersant on nano zirconia powder. *J. Eur. Ceram. Soc.*, 1999, **19**, 1725–1730.
24. Szafran, M., Jach, K., Tomaszewska-Grzeda, A. and Rokicki, G., Utilisation of enzymatic reactions in Al_2O_3 powder moulding process. *J. Therm. Anal. Calorim.*, 2003, **74**, 639–646.
25. Studart, A. R., Pandolfelli, V. C., Tervoort, E. and Gauckler, L. J., In situ coagulation of high-alumina zero-cement refractory castables. *J. Am. Ceram. Soc.*, 2002, **85**, 1947–1953.
26. Santacruz, I. and Binner, J., Rheological characterization and coagulation casting of Al_2O_3–nano zirconia suspensions. *J. Am. Ceram. Soc.*, 2008, **91**, 33–40.
27. Balzer, B., Hruschka, M. K. M. and Gauckler, L. J., Coagulation kinetics and mechanical behavior of wet alumina green bodies produced via DCC. *J. Colloid Interf. Sci.*, 1999, **216**, 379–386.
28. Graule, T. J. and Gauckler, L. J., Process for producing ceramic green bodies. *European Patent 0,605,694 V*, 1994; Graule, T. J., and Gauckler, L. J., Process for producing ceramic green bodies. *US Patent 5,667,548*, 1997.
29. Garcia-Perez, P., Pagnoux, C., Rossignol, F. and Baumard, J. F., Heterocoagulation between SiO_2 nanoparticles and Al_2O_3 submicron particles; influence of the background electrolyte. *Colloid Surf. A: Physicochem. Eng. Asp.*, 2006, **281**, 58–66.
30. Santacruz, I., Nieto, M. I., Binner, J. and Moreno, R., Gel casting of aqueous suspensions of $BaTiO_3$ nanopowders. *Ceram. Int.*, 2009, **35**, 321–326.
31. Santacruz, I., Anapoorani, K. and Binner, J., Preparation of high solids content nano zirconia suspensions. *J. Am. Ceram. Soc.*, 2008, **91**, 398–405.
32. Chevalier, J., De Aza, A. H., Fantozzi, G., Schehl, M. and Torrecillas, R., Extending the lifetime of ceramic orthopaedic implants. *Adv. Mater.*, 2000, **12**, 1619–1621.
33. Lawn, B. R., *Fracture of Brittle Solids, Second*. Cambridge University Press, Cambridge, 1993.
34. Anstis, G. R., Chantikul, P., Lawn, B. R. and Marshall, D. B., A critical evaluation of indentation techniques for measuring fracture toughness: I. Direct crack measurements. *J. Am. Ceram. Soc.*, 1981, **64**, 533–538.

35. Jiang, D., Thomson, K., Kuntz, J. D., Ager, J. W. and Mukherjee, A. K., Effect of sintering temperature on a single-wall carbon nanotube-toughened alumina-based nanocomposite. *Scripta Mater.*, 2007, **56**, 959–962.
36. Padture, N. P. and Curtin, W. A., Comment on "Effect of sintering temperature on a single-wall carbon nanotube-toughened alumina-based composite". *Scripta Mater.*, 2008, **58**, 989–990.
37. Jiang, D. and Mukherjee, A. K., Response to comment on "Effect of sintering temperature on a single-wall carbon nanotube-toughened alumina-based composite". *Scripta Mater.*, 2008, **58**, 991–993.
38. Boschini, F., Rulmont, A., Cloots, R. and Moreno, R., Colloidal stability of aqueous suspensions of barium zirconate. *J. Eur. Ceram. Soc.*, 2005, **25**, 3195–3201.
39. Moreno, R., Salomoni, A. and Mello Castanho, S., Colloidal filtration of silicon nitride aqueous slips. Part I: Optimization of the slip parameters. *J. Eur. Ceram. Soc.*, 1998, **18**, 405–416.
40. Millán, A. J., Nieto, M. I. and Moreno, R., Aqueous gel-forming of silicon nitride using carrageenans. *J. Am. Ceram. Soc.*, 2001, **84**, 62–64.
41. Gutiérrez, C. A. and Moreno, R., Interparticle potentials in nonaqueous silicon nitride suspensions. *J. Am. Ceram. Soc.*, 2003, **86**, 59–64.
42. Garmendia, N., Bilbao, L., Muñoz, R., Goikoetxea, L., García, A., Bustero, I., Olalde, B., Garagorri, N. and Obieta, I., Nanozirconia partially coated MWNT: nanostructural characterization and cytotoxicity and lixivation study. *Key Eng. Mater.*, 2008, **361–363**, 775–778.